UCHL3 plays an important role in the occurrence and development of melanoma

RUNZHI HE[1], YAJING ZHOU[2], JIANMIN LIU[3], XIAOCHONG ZHANG[4], XIAOLING ZHAO[5], LIHUI AN[6], ZIHAN LI[6] and FANG CHENG[6]

[1]The Third Department of Neurosurgery, [2]Department of Anesthesiology, [3]Department of Orthopedics, [4]Science and Education Section, [5]Tumor Laboratory, [6]Department of Dermatology, Xingtai People's Hospital, Xingtai, Hebei 054001, P.R. China

Received April 5, 2021; Accepted June 22, 2021

DOI: 10.3892/ol.2021.13017

Abstract. It has been reported that ubiquitin C-terminal hydrolase-L3 (UCHL3) plays an important role in cancer development; however, the role of UCHL3 in melanoma remains unclear. The present study aimed to investigate the role of ubiquitin C-terminal hydrolase-L3 (UCHL3) and determine its underlying molecular mechanisms in melanoma occurrence and development using *in vitro* studies. Reverse transcription-quantitative PCR analysis was performed to detect UCHL3 mRNA expression. The MTT assay was performed to assess cell proliferation. Cell apoptosis was analyzed via flow cytometry and the TUNEL assay. Cell ultrastructure was observed via transmission electron microscopy. LC3B protein expression was detected via cellular immunofluorescence, while neural precursor cell-expressed developmentally downregulated protein 8 (NEDD8) and LC3 protein expression levels, and NEDD8 ubiquitination were detected via western blot analysis. The results demonstrated that transfection with small interfering (si)RNA-UCHL3 significantly suppressed cell proliferation, whereas apoptosis was significantly enhanced, as well as autophagy, autophagosome formation and LC3B protein expression. In addition, NEDD8 protein expression and autophagosome numbers significantly decreased, while the LC3II/LC3I ratio significantly increased. NEDD8 knockdown via transfection with si-NEDD8 had similar effects to si-UCHL3, as well as si-UCHL3+ si-NEDD8. Taken together, the results of the present study suggest that UCHL3 knockdown decreases melanoma cell proliferation by increasing cell autophagy through regulating NEDD8 expression and autophagosome numbers.

Correspondence to: Dr Fang Cheng, Department of Dermatology, Xingtai People's Hospital, 16 Hongxing Street, Xingtai, Hebei 054001, P.R. China
E-mail: chengfang0127@163.com

Key words: ubiquitin C-terminal hydrolase-L3, neural precursor cell-expressed developmentally downregulated protein 8, melanoma, autophagosome, autophagy

Introduction

Melanoma is the most common malignancy of the skin, with increasing incidence rate (1). Melanoma has a high risk of metastasis. Current treatment options for melanoma primarily consist of surgical resection, radiotherapy and chemotherapy; however, these methods are only effective for tumors at early stages (2). Once metastasis occurs, the median survival time is only 6-9 months (3).

Ubiquitin C-terminal hydrolase-L3 (UCHL3) is a member of the ubiquitin carboxyl terminal hydrolase (UCH) family (4). Our previous studies have demonstrated that neural precursor cell-expressed developmentally downregulated protein (NEDD) is upregulated in melanoma tissues and cells, with associated changes in several regulatory enzymes, among which UCHL3 exhibits the most significant alterations (5,6). Recently, studies have been focusing on the role of the UCH family in cancer (7,8). Unlike other members of this family, UCHL3 not only functions as a ubiquitin hydrolase, but also regulates NEDD8 hydrolase (9). Furthermore, it acts as a cleavage enzyme of the NEDD8 precursor to promote the maturation of NEDD8 (10).

NEDD8 is a ubiquitin-like protein, and neddylation plays a key role in regulating ubiquitin ligase E3 and promoting the function of the ubiquitin pathway (11). The process of neddylation is similar to ubiquitination, which is maintained by a series of regulatory enzymes. Following transcription, NEDD8 is present in the form of its precursor, which is subsequently converted to mature NEDD8 following hydrolysis by UCHL3 hydrolase (12). Mature NEDD8 is activated by NEDD8 activase and subsequently transferred to NEDD8 ligase (13). NEDD8 carried by E2 is transferred to its substrate and associated with the cullin protein (14). However, NEDD8 hydrolase can cause an isomeric change of NEDD8, dissociating NEDD8 from cullin, which plays a negative regulatory role, a process referred to as de-neddylation (8). Thus, neddylation and de-neddylation maintain the balance by simultaneously acting on the NEDD8 protein (15). UCHL3 not only acts on the NEDD8 precursor to convert it to its mature form, but also hydrolyzes the bound NEDD8 (16). Thus, the present study aimed to investigate the effect of UCHL3 knockdown on the biological activities of melanoma cells, and determine its role in downstream NEDD8 signaling via *in vitro* cell experiments.

Materials and methods

Cell culture. Normal human epidermal cells, HaCat, were purchased from CLS Cell Lines Service GmbH, while the human melanoma cell lines, SK-MEL-2, MV3, A375 and MuM-2B were purchased from the American Type Culture Collection. Cells were maintained in DMEM (HyClone; Cytiva) supplemented with 10% fetal bovine serum (Gibco; Thermo Fisher Scientific, Inc.) and 1% penicillin-streptomycin (Gibco; Thermo Fisher Scientific, Inc.), at 37˚C with 5% CO_2.

Small interfering (si)RNA transfection. One day prior to transfection, SK-MEL-2 and A375 cells ($1x10^5$) were seeded into the 6-well cell culture plate and cultured until they reached a confluence of 70-80%. Serum-free Opti-MEM (Sigma-Aldrich; Merck KGaA, 125 μl) was used to dilute 5 μl 20 μM siRNA and negative control (NC), which were gently mixed and incubated at room temperature for 5 min. Subsequently, serum-free Opti-MEM (125 μl) was used to dilute 5 μl Lipofectamine® (lipo)3,000 (cat. no. L300001; Invitrogen; Thermo Fisher Scientific, Inc.), which was gently mixed and incubated for 5 min at room temperature. The solutions were incubated for an additional for 20 min at room temperature. The plasmid-lipo3,000 mixture was added into culture wells of the 750 μl complete culture medium containing $1x10^5$ cells for complete mixing, and the culture plates were incubated at 37˚C for 48 h with 5% CO_2. The following sequences were used for transfection: NC forward, 5'-UGACCUACAACUUCUAUGGTT-3' and reverse, 5'-UUCUCCGAACGUGUCACGUTT-3'; UCHL3 (human) siRNA-1 forward, 5'-GAACAGAAGAGGAAGAAAATT-3' and reverse, 5'-UUUUCUUCCUCUUCUGUUCTT-3'; UCHL3 (human) siRNA-2 forward, 5'-CUGAAGAACGAGCCAGAUATT-3' and reverse, 5'-UAUCUGGCUCGUUCUUCAGTT-3'; UCHL3 (human) siRNA-3 forward, 5'-UGGAACAAUUGGACUGAUUTT-3' and reverse, 5'-AAUCAGUCCAAUUGUUCCATT-3'; NEDD8 (human) siRNA-1 forward, 5'-CAGACAAGGUGGAGCGAAUTT-3' and reverse, 5'-AUUCGCUCCACCUUGUCUGTT-3'; NEDD8 (human) siRNA-2 forward, 5'-CGGAAAGGAGAUUGAGAUUTT-3' and reverse, 5'-AAUCUCAAUCUCCUUUCCGTT-3'; and NEDD8 (human) siRNA-3 forward, 5'-UGGAGGAGAAAGAGGGAAUTT-3' and reverse, 5'-AUUCCCUCUUUCUCCUCCATT-3'.

MTT assay. Cells in the NC group were treated with normal medium; cells in the si-NC groups were transfected with si-NC; cells in the si-UCHL3 group were transfected with si-UCHL3, which inhibited UCHL3 expression; cells in the si-NEDD8 group were transfected with si-NEDD8, which inhibited NEDD8 expression; and cells in the si-UCHL3+ si-NEDD8 group were transfected with si-UCHL3 and si-NEDD8.

Following treatment for 48 h, 20 μl MTT solution (5 g/l; Amresco, LLC) was added and cells were incubated for an additional 4 h at 37˚C. The excessive culture medium was discarded and 150 μl DMSO was added for 10 min of oscillatory reaction. Absorbance (OD value) was detected at a wavelength of 490 nm, using a microplate reader (BioTek ELx800). The cell proliferation rate was calculated in each group.

Apoptosis analysis. Cells in each group were digested with EDTA-free trypsin (Sigma-Aldrich; Merck KGaA) centrifuged at 8,000 x g for 30 sec at 4˚C, collected, rinsed twice with PBS and resuspended in binding buffer (Sigma-Aldrich; Merck KGaA) ($1x10^5$ cells/l). Cells were subsequently stained with Annexin V-FITC and PI for 10 min at 4˚C in the dark, according to the manufacturer's instructions (Nanjing KeyGen Biotech Co., Ltd.). Fluorescence intensity was measured at an excitation wavelength of 488 nm and emission wavelength of 530 nm, using a flow cytometer (Becton-Dickinson and Company). The experiment was performed in triplicate.

Reverse transcription-quantitative (RT-q)PCR. Following the corresponding treatments in each group for 48 h, total RNA was extracted from cells of different groups using TRIzol® reagent (Thermo Fisher Scientific, Inc.), according to the manufacturer's instructions. The purity and concentration of RNA were detected using microNucleic Acid Analyzer (Thermo Fisher Scientific, Inc.). RNA was reverse transcribed into cDNA using the Takara reverse transcription kit (Takara Biotechnology Co., Ltd.), at 30˚C for 10 min, 42˚C for 30 min, 99˚C for 5 min and 4˚C for 5 min. qPCR was subsequently performed using the Takara fluorescent quantitative kit (Takara Biotechnology Co., Ltd.), according to the manufacturer's instructions. GAPDH was used as the internal reference for PCR amplification. A DNA Engine with a Chromo 4 detector (MJ Research, Inc.; Bio-Rad Laboratories, Inc.) was used for qPCR. The following thermocycling conditions were used for qPCR: 95˚C for 30 sec, 60˚C for 30 sec and 72˚C for 30 sec for a total of 40 cycles, followed by extension at 60˚C for 5 min. Relative expression levels were calculated using the $2^{-\Delta\Delta Cq}$ method (12). The primer sequences used for qPCR were designed and synthesized by Shanghai Shenggong Biology Engineering Technology Service, Ltd. The following primer sequences were used for qPCR: GAPDH forward, 5'-GGTGAAGGTCGGTGTGAACG-3' and reverse, 5'-GCTCCTGGAAGATGGTGATGG-3'; UCHL3 forward, 5'-AGCCCTGAAGAACGAGCCAGAT-3' and reverse, 5'-ACTTGGTGCCTCAGTCTGACCT-3'; NEDD8 forward, 5'-AATCAAGGAGCGTGTGGAGGAG-3' and reverse, 5'-AGAGCCAACACCAGGTGAAGGA-3'; and LC3B forward, 5'-TCAGCGTCTCCACACCAATCTCA-3' and reverse, 5'-CGAACGTCTCCTGGGAGGCATA-3'. The amplification conditions were as follows: Initial denaturation at 50˚C for 2 min, 95˚C for 5 min, followed by 50 cycles of 95˚C for 15 sec and 60˚C for 30 sec. The experiment was repeated in triplicate.

TUNEL assay. SK-MEL-2 and A375 cells in each group were treated with the corresponding treatments for 48 h. Cells were subsequently fixed in 4% paraformaldehyde at room temperature for 25 min and washed twice with PBS. Cells were permeabilized with 0.2% Triton X-100 for 5 min, washed twice with PBS, treated with fresh 3% H_2O_2 at room temperature for 5 min, followed by another two washes with PBS. After the slides were dried, 50 μl TUNEL reaction mixture (TdT and dUTP mixed at a ratio of 1:9) was added to the cells at 37˚C for 1 h. Only 50 μl dUTP solution was added to the NC group, and the reaction time was 60 min at 37˚C in a wet box in the dark. After washing three times with PBS, 50 μl converter-POD was added to the cells after drying the slides for 30 min at 37˚C in a wet box in the dark. Subsequently, 100 μl DAB developer was added for 10 min at room temperature after washing three time with PBS. After

another three washes with PBS, cells were re-stained with hematoxylin, immediately washed with tap water after 30 sec of reaction, dehydrated with gradient alcohol, transparentized with xylene and sealed with neutral gum. The ratio of positive cells was observed under a fluorescence microscope (Olympus Corporation BX43; magnification, x200).

Observation of cellular ultrastructure under a transmission electron microscope (TEM). Following the corresponding treatments in each group for 48 h, cells were collected via centrifugation at 1,000 x g for 10 min at room temperature. After washing three times with PBS, cells were immediately fixed with 25 g/l glutaraldehyde overnight at 4˚C. Subsequently, cells were fixed with 10 g osmium tetroxide for 2 h at 4˚C, dehydrated with gradient ethanol, soaked and embedded with Epon812 epoxy resin at 4˚C for 2 h, followed by semi-ultrathin slicing (80 nm), as well as double staining with uranium acetate and lead citrate at 4˚C for 2 h. Cells were observed and photographed under a Hitachi H-600 TEM (Hitachi, Ltd.).

Detection of LC3B protein expression in cells under a laser confocal microscope. Following the corresponding treatments in each group for 48 h, cells were fixed with 4% paraformaldehyde at room temperature for 10 min. After washing three times with PBS (5 min each), cells were lysed using 0.1% Triton-100 (Nanjing KeyGen Biotech Co., Ltd.) for 20 min. After re-washing three times with PBS (5 min each), 5% BSA (Sigma-Aldrich; Merck KGaA) was added for sealing at room temperature for 20 min. Subsequently, rabbit anti-mouse LC3B monoclonal antibody (cat. no. ab205718; Abcam; 1:100) was added and incubated overnight at 4˚C, followed by washing three times with PBS (5 min each). Following the primary incubation, samples were incubated with HRP-labeled goat anti-rabbit IgG (cat. no. ab192890; Abcam; 1:500) at 37˚C for 45 min, in the dark. Cells were washed with PBS, and Hochest 33342 dye (1:200; Nanjing KeyGen Biotech Co., Ltd.) was used to stain the nuclei for 5 min at room temperature, and the treated cells were subsequently washed with PBS. Cells were observed and photographed under a laser confocal microscope (magnification, x200). Mean fluorescence intensity was detected using ImageJ software v1.8.0.112 (National Institutes of Health). The experiment was performed in triplicate.

Western blotting. Total protein from each group was extracted from cells using the total protein extraction kit (cat. no. KGP250; Nanjing KeyGen Biotech Co., Ltd.), according to the manufacturer's instructions. The BCA protein concentration assay kit was used to detect total protein concentration and calculate the loading amount. Following denaturation by heating at 100˚C, 30 μg of total protein was loaded per lane. The proteins were separated by 10% SDS-PAGE, transferred onto PVDF membranes and blocked with 5% skimmed milk at room temperature for 1 h, followed by three washes in 20% TBST (5 min each). The membranes were incubated with primary antibodies against NEDD8 (1:2,000; cat. no. ab81264; Abcam), LC3 (1:2,000; cat. no. ab192890; Abcam) and UCHL3 (cat. no. ab126621; Abcam; 1:2,000) overnight at 4˚C. Membranes were washed three times with TBS-0.5% Tween-20 (TBS-T) and subsequently incubated with diluted goat anti-Rabbit IgG-HRP secondary antibody (1:500; cat. no. KGAA35; Nanjing KeyGen Biotech Co., Ltd.) for 2 h at room temperature. Membranes were re-washed, placed into a clean culture dish and evenly smeared with ECL development solution (cat. no. KGP116; Nanjing KeyGen Biotech Co., Ltd.) prepared at a ratio of 1:1. Membranes were exposed in the Bio-Rad exposure system (cat. no. 170-4150; Bio-Rad Laboratories, Inc.), using ImageJ software (version 1.52r; National Institutes of Health) for image acquisition.

Statistical analysis. Statistical analysis was performed using SPSS 19.0 software (IBM Corp.). Measurement data are consistent with normal distribution. All experiments were performed in triplicate and data are presented as the mean ± SD. One-way ANOVA followed by Tukey's post hoc test were used to compare differences among multiple groups. $P<0.05$ was considered to indicate a statistically significant difference.

Results

UCHL3 gene expression in cells of each group. As presented in Fig. 1A, UCHL3 expression was significantly higher in the melanoma cell lines, SK-MEL-2, MV-3, A375 and MUN2B (all $P<0.001$) compared with normal HaCat cells. Among these, SK-MEL-2 and A375 cells exhibited the highest expression of UCHL3, and thus were selected for subsequent experimentation. To assess the effect of UCHL3 inhibition, si-UCHL3-1, si-UCHL3-2 and si-UCHL3-3 were transfected into SK-MEL-2 and A375 cells. The results demonstrated that UCHL3 expression significantly decreased in all groups compared with the si-NC group (all $P<0.01$; Fig. 1B), particularly in the si-UCHL3-2 group. Thus, si-UCHL3-2 was selected for UCHL-3 knockdown experiments.

Effect of UCHL3 knockdown on the proliferation of melanoma cells. The results of the MTT assay demonstrated no significant differences in the proliferation rate of A375 and SK-MEL-2 cells between the si-NC and NC groups ($P>0.05$), while the proliferation rate significantly decreased in the si-UCHL3 group on days 2, 3 and 4 (all $P<0.05$; Fig. 1C).

Effect of UCHL3 knockdown on the apoptosis of melanoma cells. Flow cytometric analysis demonstrated no significant differences in the apoptotic rates of A375 and SK-MEL-2 cells between the si-NC and NC groups ($P>0.05$). However, the apoptotic rates significantly increased in the si-UCHL3 group of both cell lines compared with NC group ($P<0.001$; Fig. 2A and B).

TUNEL staining analysis exhibited no significant differences in the number of apoptotic A375 and SK-MEL-2 cells between the NC and si-NC groups ($P>0.05$), while a significant increase in the number of apoptotic cells was observed in the si-UCHL3 group compared with the NC group ($P<0.001$; Fig. 2C and D).

Effect of UCHL3 knockdown on the ultrastructure and LC3B protein expression of melanoma cells. No significant changes in the ultrastructure of A375 and SK-MEL-2 cells were observed between the NC and si-NC groups, while the number of autophagosomes increased in A375 and SK-MEL-2 cells in the si-UCHL3 group (Fig. 3A and B), suggesting that UCHL3 knockdown may enhance autophagy.

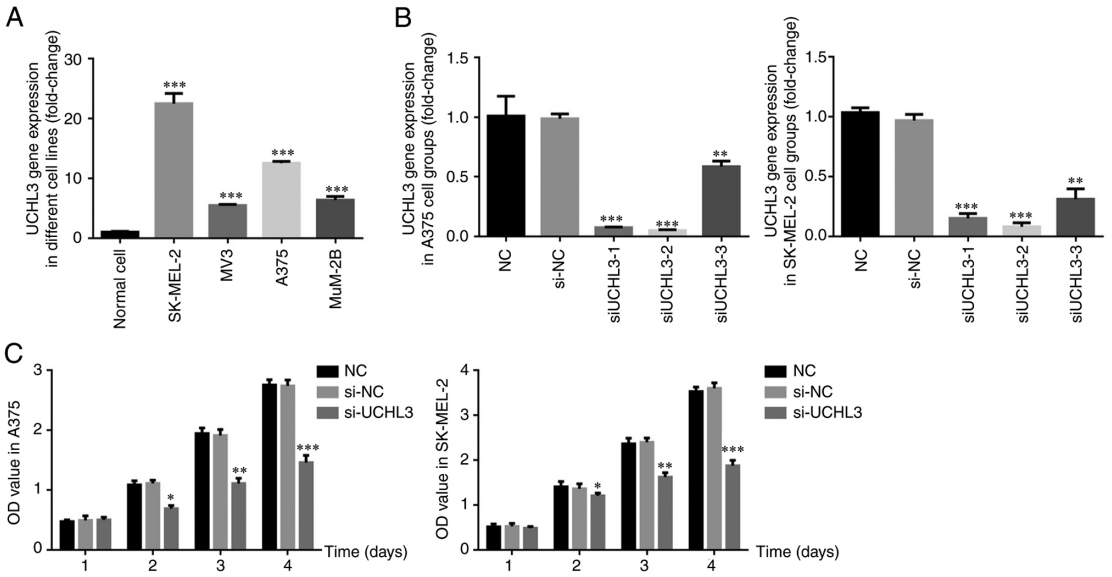

Figure 1. UCHL3 gene expression in cells of each group and cell proliferation rate of different cell groups. (A) UCHL3 gene expression in different cell lines. (B) UCHL3 gene expression in SK-MEL-2 and A375 cells. (C) Cell proliferation rate of different A375 and SK-MEL-2 cell groups. UCHL3, ubiquitin C-terminal hydrolase-L3; NC, negative control; si, small interfering; OD, optical density. *P<0.05, **P<0.01 vs. normal control group; ***P<0.001 vs. HaCat cells or normal control group.

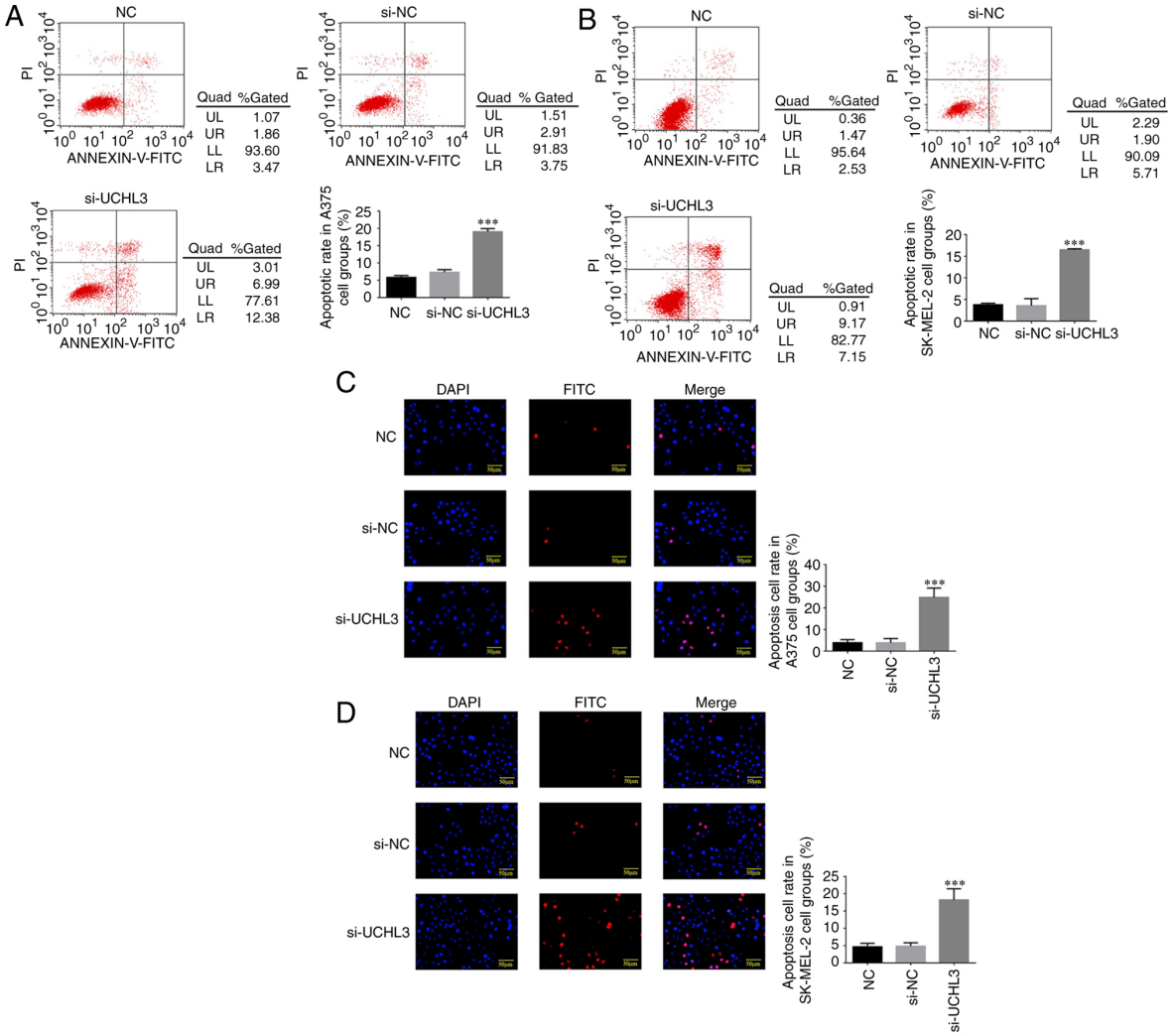

Figure 2. Effect of UCHL3 knockdown on the apoptosis of melanoma cells. (A) Apoptotic rates of (A) A375 and (B) SK-MEL-2 cell groups via flow cytometry. (C) Apoptotic rates of (C) A375 and (D) SK-MEL-2 cell groups via the TUNEL assay (magnification, x200). ***P<0.001 vs. normal control group. UCHL3, ubiquitin C-terminal hydrolase-L3; NC, negative control; si, small interfering.

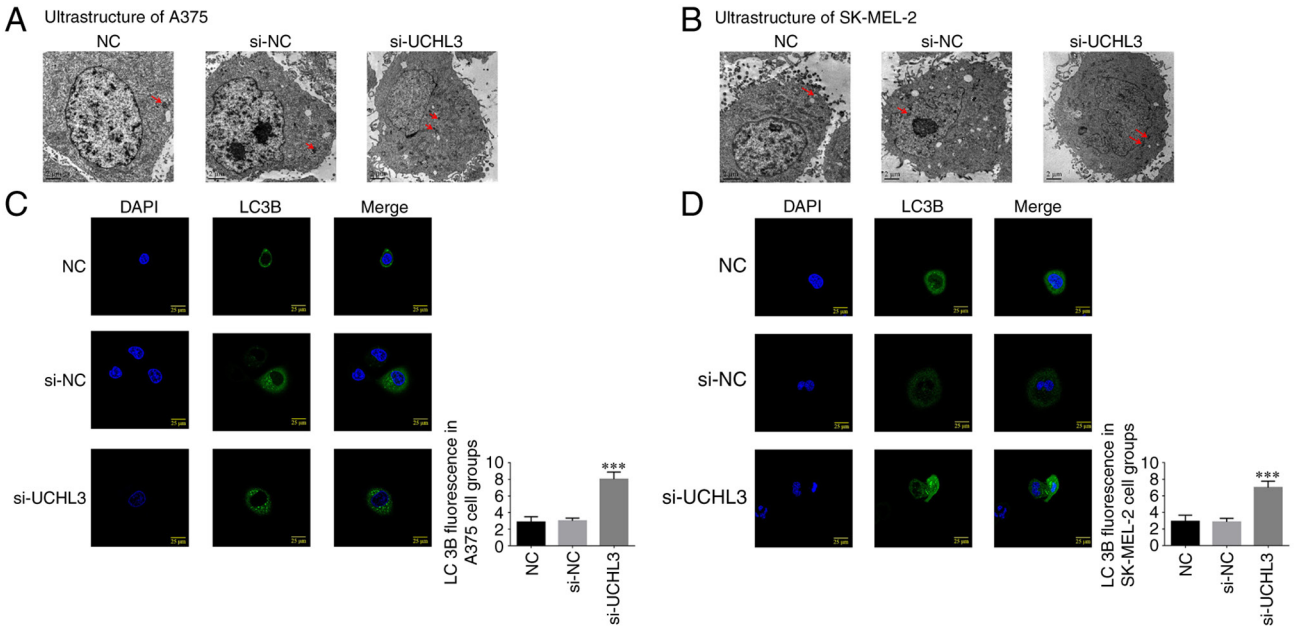

Figure 3. Effect of UCHL3 knockdown on the ultrastructure and LC3B protein expression of melanoma cells. Ultrastructure of (A) A375 and (B) SK-MEL-2 cell groups via transmission electron microscopy. LC3B protein expression in (C) A375 and (D) SK-MEL-2 cell groups (magnification, x400). Arrows depict autophagosome. ***P<0.001 vs. normal control group. UCHL3, ubiquitin C-terminal hydrolase-L3; NC, negative control; si, small interfering.

Immunofluorescence analysis demonstrated no significant differences in LC3B protein expression in A375 and SK-MEL-2 cells between the NC and si-NC groups (P>0.05); however, UCHL3 knockdown significantly increased LC3B protein expression in the si-UCHL3 group compared with the NC group (P<0.001; Fig. 3C and D).

Effect of UCHL3 knockdown on relevant gene expression in melanoma cells. RT-qPCR analysis demonstrated no significant differences in UCHL3, NEDD8 and LC3B expression levels between the NC and si-NC groups (P>0.05; Fig. 4A and B); however, UCHL3 knockdown significantly decreased the expression levels of UCHL3 and NEDD8, and significantly increased LC3B expression in the si-UCHL3 group compared with the NC group (all P<0.001; Fig. 4A and B).

Effect of UCHL3 knockdown on relevant protein expression and NEDD8 ubiquitination. Western blot analysis demonstrated no significant differences in NEDD8 protein expression, the LC3II/LC3I ratio and NEDD8 ubiquitination in A375 and SK-MEL-2 cells between the NC and si-NC groups (all P>0.05; Fig. 5A and B). However, UCHL3 knockdown significantly decreased NEDD8 protein expression and markedly increased the LC3II/LC3I ratio in the si-UCHL3 group compared with the NC group (all P<0.001; Fig. 5A), accompanied by notably decreased NEDD8 ubiquitination (Fig. 5B).

Sequence screening for NEDD8 knockdown and corresponding expression in each group. RT-qPCR analysis demonstrated no significant differences in NEDD8 gene expression between the si-NC and NC groups (P>0.05; Fig. 6A). Following transfection with three si-NEDD8 sequences, NEDD8 gene expression significantly decreased in the si-NEDD8 groups compared with the NC group (all P<0.01; Fig. 6A), with the most significant decrease observed in the si-NEDD8-3 group. Thus, the si-NEDD8-3 sequence was used for subsequent experimentation.

Notably, the proliferation of A375 and SK-MEL-2 cells on days 2, 3 and 4 significantly decreased in the si-UCHL3, si-NEDD8 and si-UCHL3+ si-NEDD8 groups compared with the NC group (all P<0.05; Fig. 6B).

Detection of cell apoptosis in each group. Flow cytometric analysis demonstrated that the apoptotic rates of A375 and SK-MEL-2 cells significantly increased in the si-UCHL3, si-NEDD8 and si-UCHL3+ si-NEDD8 groups compared with the NC group (all P<0.001; Fig. 7A and B), while no significance differences were observed between the si-UCHL3, si-NEDD8 and si-UCHL3+ si-NEDD8 groups (P>0.05).

Detection of apoptotic cell count in each group. The results of the TUNEL assay demonstrated that the apoptotic rates of A375 and SK-MEL-2 cells significantly increased in the si-UCHL3, si-NEDD8 and si-UCHL3+ si-NEDD8 groups compared with the NC group (all P<0.001; Fig. 8A and B). However, no significant differences were observed between the si-UCHL3, si-NEDD8 and si-UCHL3+ si-NEDD8 groups (P>0.05).

Ultrastructure of melanoma cells and LC3B protein expression. TEM analysis demonstrated no nuclear damage or autophagosome formation in A375 and SK-MEL-2 cells in the NC and si-NC groups, while autophagosomes were observed in cells in the si-UCHL3, si-NEDD8 and si-UCHL3+ si-NEDD8 groups (Fig. 9A and B).

Immunofluorescence analysis demonstrated that LC3B protein expression in A375 and SK-MEL-2 cells was relatively lower in the NC and si-NC groups. Furthermore, LC3B

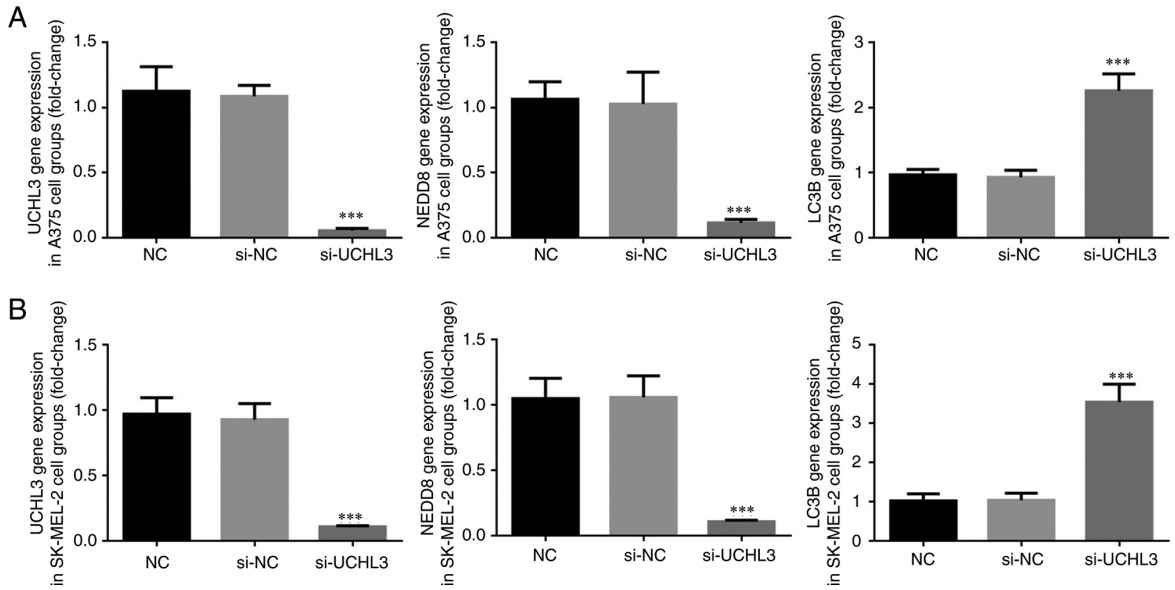

Figure 4. Effect of UCHL3 knockdown on relevant gene expression in melanoma cells. Reverse transcription-quantitative PCR analysis was performed to detect gene expression levels in (A) A375 and (B) SK-MEL-2 cell groups. ***P<0.001 vs. normal control group. UCHL3, ubiquitin C-terminal hydrolase-L3; NEDD8, neural precursor cell-expressed developmentally downregulated protein 8; NC, negative control; si, small interfering.

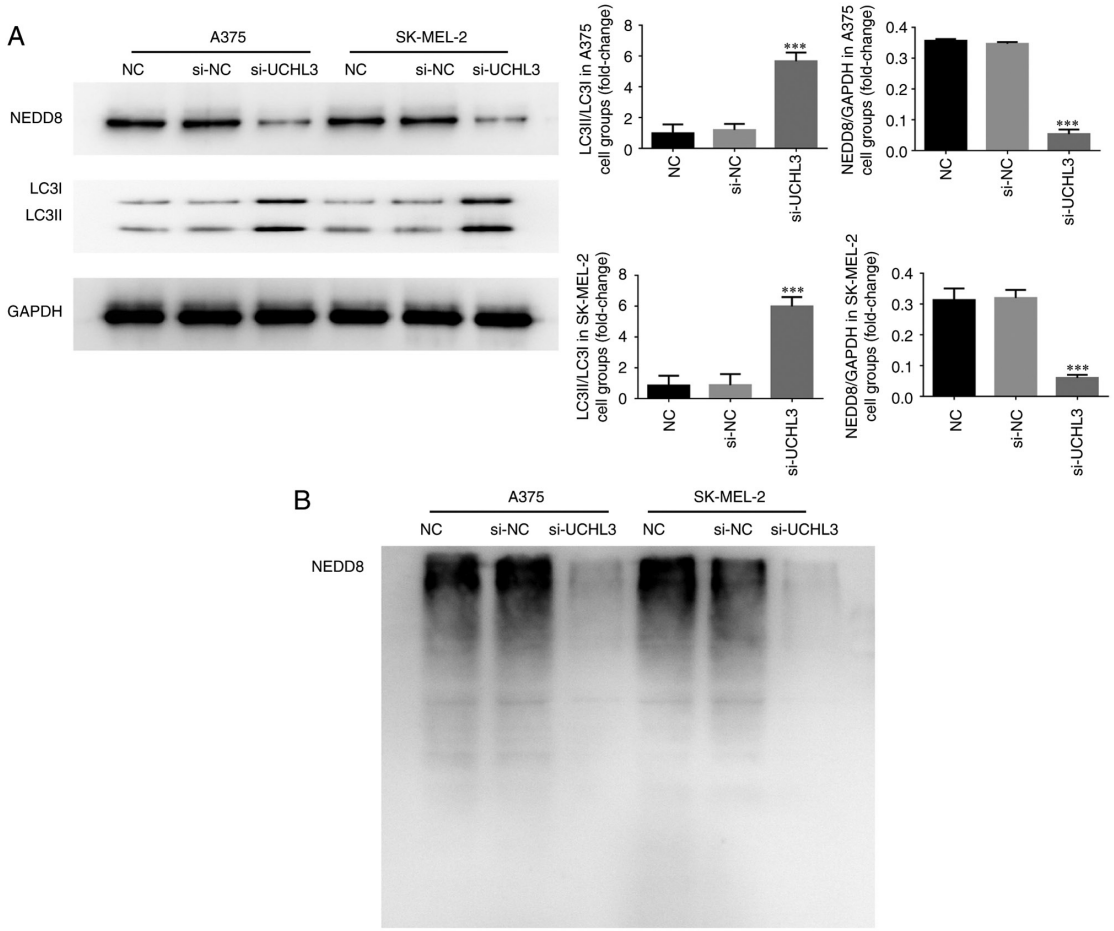

Figure 5. Effect of UCHL3 knockdown on relevant protein expression and NEDD8 ubiquitination. (A) NEDD8 and LC3 protein expression levels were detected via western blotting. (B) NEDD8 ubiquitination. ***P<0.001 vs. normal control group. UCHL3, ubiquitin C-terminal hydrolase-L3; NEDD8, neural precursor cell-expressed developmentally downregulated protein 8; NC, negative control; si, small interfering.

protein expression was significantly higher in the si-UCHL3, si-NEDD8 and si-UCHL3+ si-NEDD8 groups compared with the NC group (all P<0.001; Fig. 9C and D), while no significant differences were observed among the three groups (P>0.05).

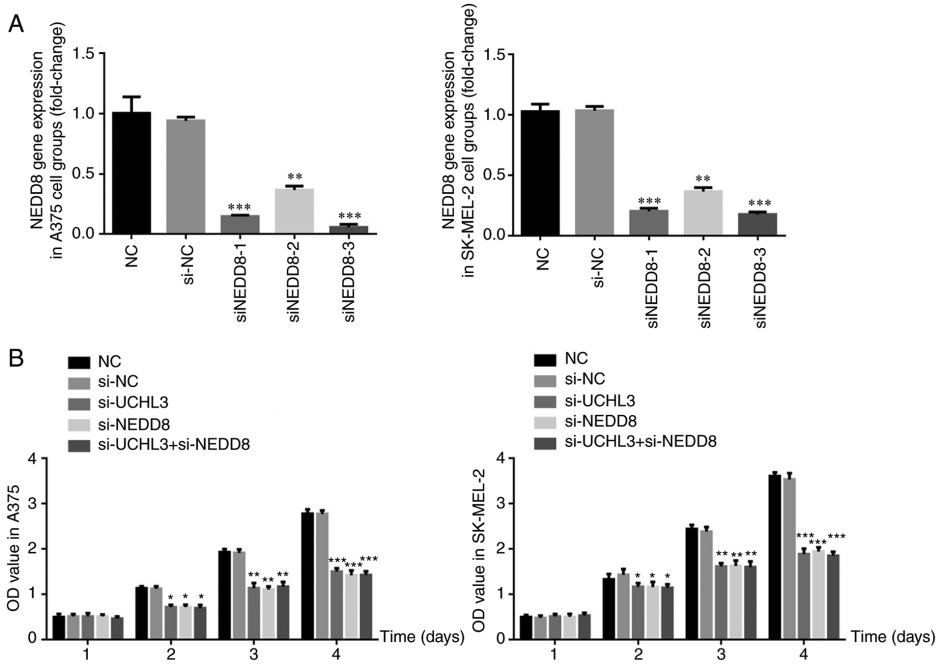

Figure 6. Sequence screening for NEDD8 knockdown and corresponding expression in each group. (A) Reverse transcription-quantitative PCR analysis was performed to detect NEDD8 gene expression in the different groups. (B) Cell proliferation rates of the different groups. *P<0.05, **P<0.01 and ***P<0.001 vs. normal control group. NEDD8, neural precursor cell-expressed developmentally downregulated protein 8; UCHL3, ubiquitin C-terminal hydrolase-L3; NC, negative control; si, small interfering; OD, optical density.

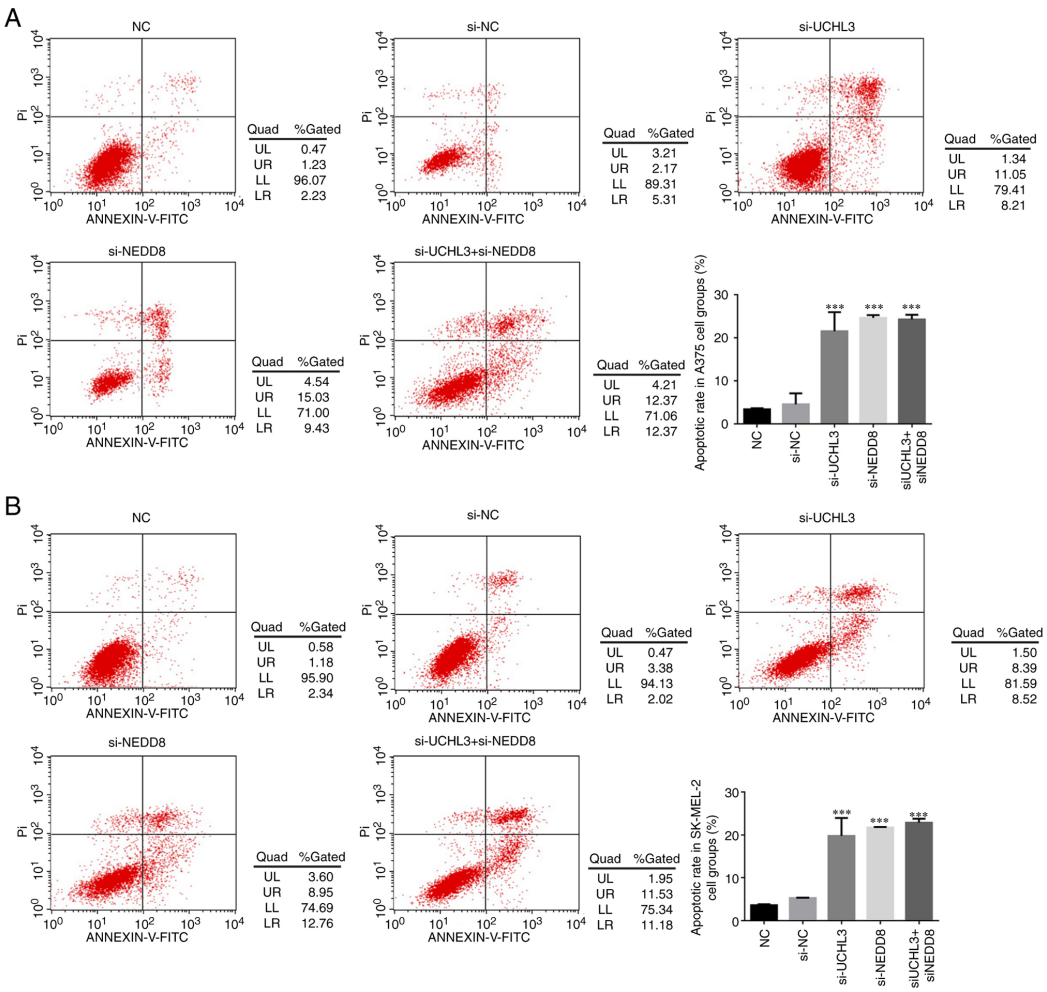

Figure 7. Detection of cell apoptotic rates in each group. Apoptotic rates in (A) A375 and (B) SK-MEL-2 cell groups. ***P<0.001 vs. normal control group. UCHL3, ubiquitin C-terminal hydrolase-L3; NEDD8, neural precursor cell-expressed developmentally downregulated protein 8; NC, negative control; si, small interfering.

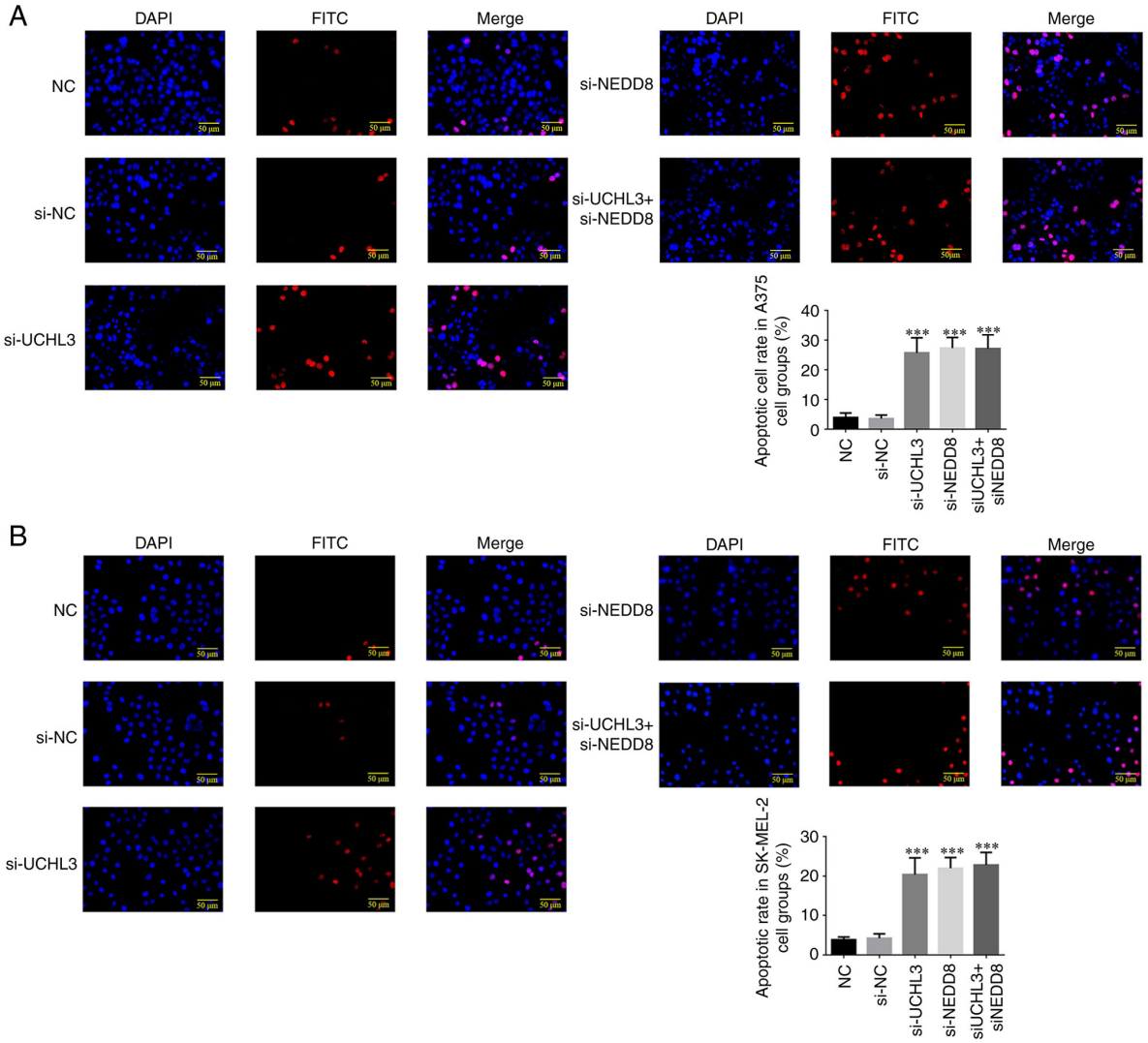

Figure 8. Detection of apoptotic cell count in each group. Apoptotic cell rates in (A) A375 and (B) SK-MEL-2 cell groups were measured via the TUNEL assay (magnification, x200). ***P<0.001 vs. normal control group. UCHL3, ubiquitin C-terminal hydrolase-L3; NEDD8, neural precursor cell-expressed developmentally downregulated protein 8; NC, negative control; si, small interfering.

UCHL3 and NEDD8 gene expression levels. RT-qPCR analysis demonstrated no significant differences in UCHL3 and NEDD8 gene expression levels in A375 and SK-MEL-2 cells between the si-NC and NC groups (P>0.05; Fig. 10). However, UCHL3 expression significantly decreased in the si-UCHL3 and si-UHL3+ si-NEDD8 groups (all P<0.001; Fig. 10A and B), while NEDD8 gene expression significantly decreased in the si-UCHL3, si-NEDD8 and si-UCHL3+ si-NEDD8 groups (all P<0.001; Fig. 10A and B).

Detection of relevant protein expression and NEDD8 ubiquitination. Western blot analysis demonstrated no significant differences in NEDD8 protein expression, the LC3II/LC3I ratio and NEDD8 ubiquitination in A375 and SK-MEL-2 cells between the NC and si-NC groups (P>0.05, Fig. 11A and B). Notably, NEDD8 protein expression significantly decreased and the LC3II/LC3I ratio increased in the si-UCHL3, si-NEDD8 and si-UCHL3+ si-NEDD8 groups compared with the NC group (all P<0.001; Fig. 11A), with no significant differences among the three groups. In addition, NEDD8 ubiquitination was significantly suppressed in the si-UCHL3, si-NEDD8 and si-UCHL3+ si-NEDD8 groups (Fig. 11B). Notably, UCHL3 protein expression significantly decreased in the si-UCHL3 and si-UCHL3+si-NEDD8 groups compared with the NC group (all P<0.001; Fig. 11A).

Discussion

UCHL3 is a member of the UCH family, which has attracted recent interest in tumor research (17). Among the UCH family members, UCHL1 is the most extensively investigated in the context of several malignancies, including esophageal cancer (18), gastric cancer (19), renal cancer (20), prostate cancer (21) and ovarian cancer (13). UCHL1 mainly functions as a ubiquitin hydrolase and ubiquitin ligase, and has limited distribution, primarily in the ovary, testis and neurons (22). A previous study demonstrated that UCHL3 can regulate DNA repair, and thus may participate in tumor development (23). It has been reported that interference with UCHL3 may cause meiotic arrest of mature oocytes (24,25). Downregulating UCHL3 expression in metastatic prostate cancer may interfere with UCHL3 expression in normal prostate cells and

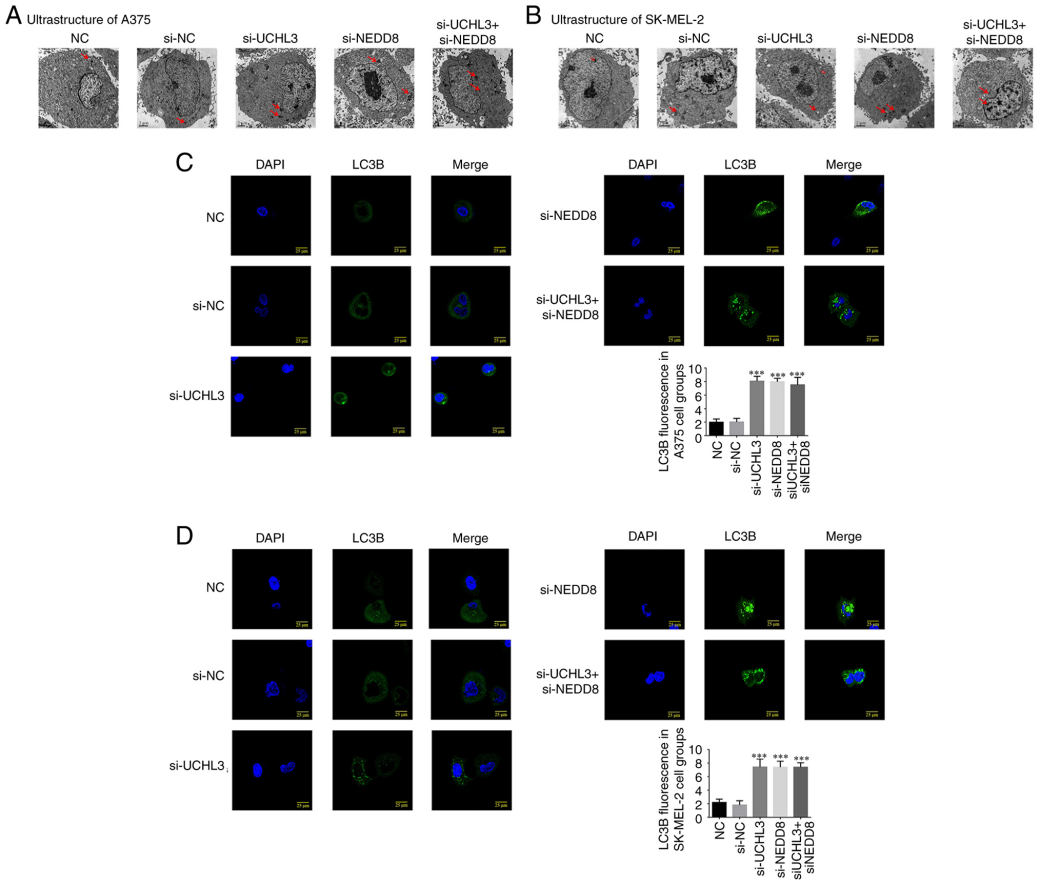

Figure 9. Ultrastructure of melanoma cells and LC3B protein expression in each group. Ultrastructure of (A) A375 and (B) SK-MEL-2 cell groups via transmission electron microscopy. LC3B protein expression in (C) A375 and (D) SK-MEL-2 cell groups (magnification, x400). Arrows indicate autophagosome. ***P<0.001 vs. normal control group. UCHL3, ubiquitin C-terminal hydrolase-L3; NEDD8, neural precursor cell-expressed developmentally downregulated protein 8; NC, negative control; si, small interfering.

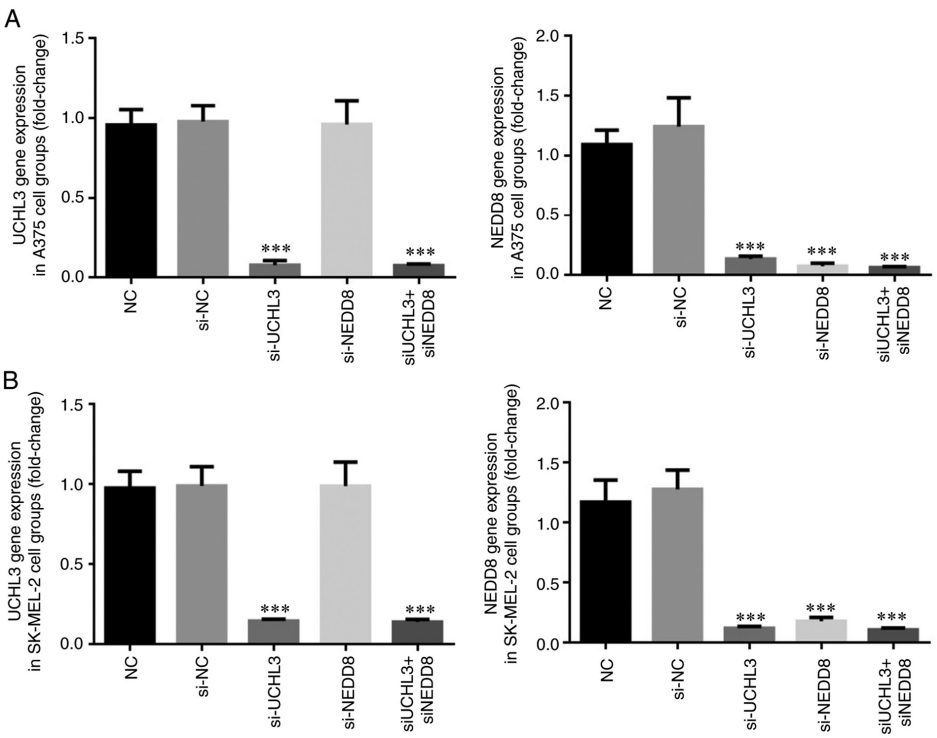

Figure 10. UCHL3 and NEDD8 gene expression levels in each group. Relative gene expression levels in different (A) A375 and (B) SK-MEL-2 cell groups. ***P<0.001 vs. normal control group. UCHL3, ubiquitin C-terminal hydrolase-L3; NEDD8, neural precursor cell-expressed developmentally downregulated protein 8; NC, negative control; si, small interfering.

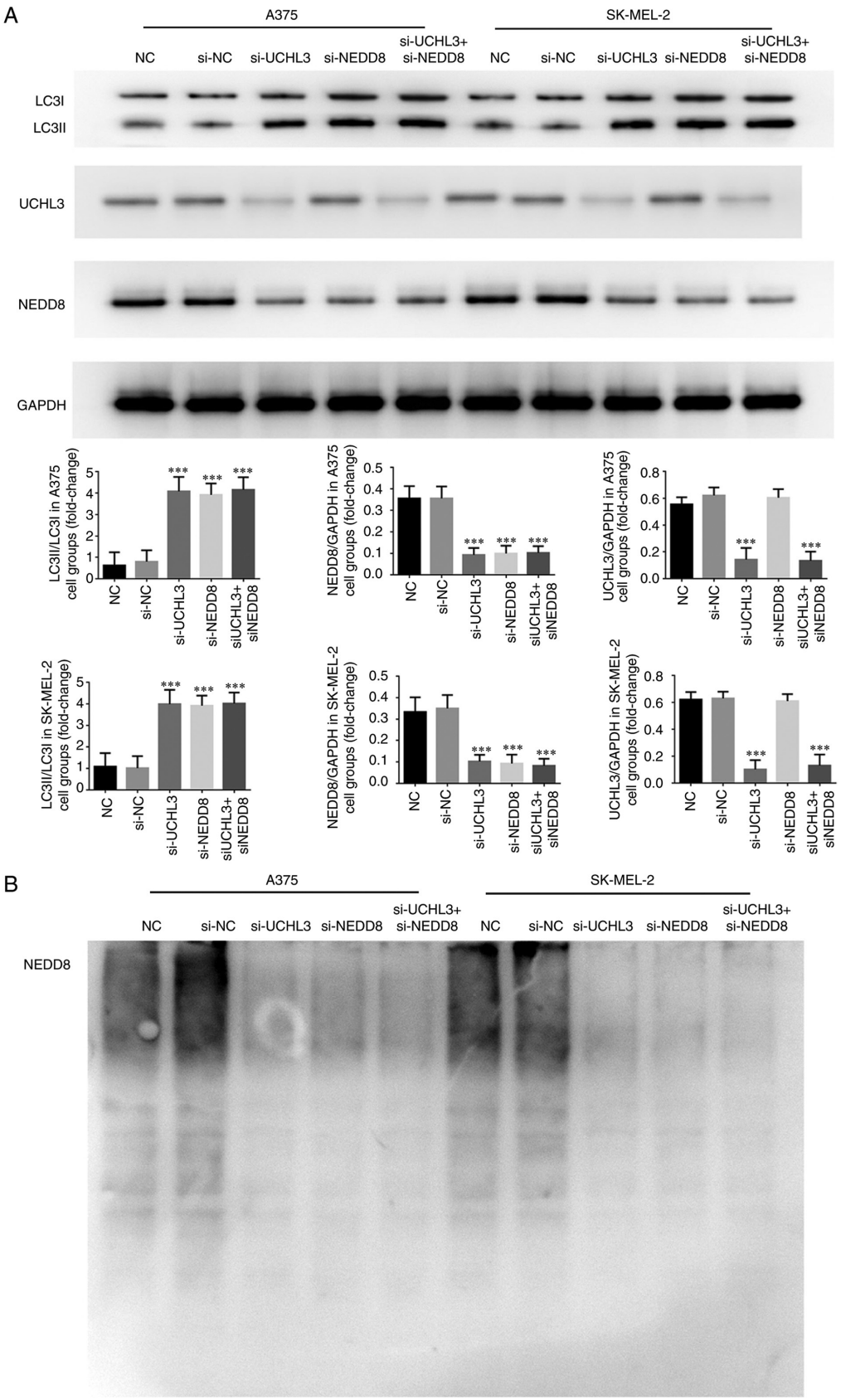

Figure 11. Detection of relevant protein expression and NEDD8 ubiquitination. (A) NEDD8 and LC3 protein expression levels. (B) NEDD8 ubiquitination. ***P<0.001 vs. normal control group. NEDD8, neural precursor cell-expressed developmentally downregulated protein 8; UCHL3, ubiquitin C-terminal hydrolase-L3; NC, negative control; si, small interfering.

promote their migratory and invasive abilities (7). UCHL3 expression is upregulated in breast cancer (26) and cervical cancer (27), and it may be involved in the occurrence and malignant behavior of these two malignancies. Thus, whether

UCHL3 acts as an oncogene or tumor suppressor varies across different tumors.

The results of the present study demonstrated that UCHL3 was highly expressed in melanoma cell lines (SK-MEL-2, MV3, A375 and MuM-2B), and UCHL3 mRNA expression was upregulated in SK-MEL-2 and A375 cell lines. Thus, SK-MEL-2 and A375 cell lines were selected for subsequent experimentation. The biological activities (cell proliferation, invasion and migration) of A375 and SK-MEL-2 melanoma cells were significantly inhibited following UCHL3 knockdown. Taken together, these results suggest that abnormally high UCHL3 expression may be an important factor in melanoma, and its knockdown may effectively inhibit the occurrence and development of melanoma.

Autophagy is another important pathway for protein degradation. Autophagy is widely present in eukaryotic cells, where it plays a key role in degrading longevity-related proteins and organelles, and is important for maintaining cell stability (28). In addition, autophagy is a natural process in cells that enables self-digestion of intracellular elements (29). Under conditions of injury, autophagy can provide energy through lysosome digestion of its own contents to maintain cell survival (30). Under normal physiological conditions, autophagy is maintained at basic levels; however, it is notably enhanced under conditions of nutrient deficiency, growth factor deficiency, hypoxia and other stress conditions (31). Furthermore, autophagy is an important cell process involved in cell proliferation, differentiation, senescence and immunity (30). Disordered autophagy has been reported in multiple diseases, such as infections (32), neurodegenerative conditions (33), cardiovascular diseases (34), metabolic diseases (35) and tumors (36,37). Autophagy may play a role in tumors in an environment-dependent manner. Conversely, it can destroy damaged organelles, cause cell aging and inhibit the proliferation of precancerous cells, exhibiting a tumor-inhibiting effect (28). It can also provide nutrients for tumor cells under conditions of nutritional and oxygen deficiency, thus promoting tumor progression (38). Autophagy also plays different roles in the development of melanoma. For example, a previous study reported a lower level of autophagy in the tumor specimens of 194 patients with early melanoma compared with benign nevus (39). Another study revealed that patients with melanoma with higher autophagy levels may have a longer progression-free survival time (40), while nodular melanoma with low autophagy levels is associated with an increased risk of ulceration and tumor invasion, accompanied by a low 5-year survival rate following surgery (41), suggesting that autophagy may inhibit melanoma growth. Conversely, another study on superficial spreading melanoma reported that the autophagy level was higher in tumor tissues compared with normal melanocytes (39). In addition, the level of autophagy is higher in metastatic melanoma compared with primary tumor (42). In a previous study, UCHL3 knockdown increased the number of autophagosomes on examination of the ultrastructure of melanoma cells, which was associated with a notable increase in LC3B levels and the LC3II/LC3I ratio (43). The results of the present study suggest that the increase in autophagy level may be an important factor mediating the inhibitory effects of UCHL3 knockdown on the biological activity of melanoma cells.

Ubiquitination is closely associated with autophagy (44,45). The results of the present study demonstrated that UCHL3 knockdown in melanoma cells not only inhibited NEDD8 expression, but also decreased the ubiquitination of NEDD8. Furthermore, autophagy was significantly enhanced along with the decrease in NEDD8 ubiquitination.

In conclusion, the results of the present study demonstrated that UCHL3 knockdown decreased melanoma cell proliferation by increasing cell autophagy through regulating NEDD8 expression and autophagosome numbers *in vitro*. However, the present study is not without limitations as it only focused on the effect of UCHL3 on melanoma *in vitro*, whereas its effects *in vivo* remain unclear. Thus, this will be the focus of prospective studies. In addition, future studies will aim to assess the effect of UCHL3 on other melanoma cell lines.

Acknowledgements

Not applicable.

Funding

No funding was received.

Availability of data and materials

The datasets used or analyzed during the current study are available from the corresponding author upon reasonable request.

Authors' contributions

RH, YZ, JL and FC conceptualized and designed the present study. RH, YZ, JL, XCZ, XLZ, LA and ZL performed the experiments. XCZ, XLZ, LA and ZL analyzed the data. RH, YZ and JL drafted the initial manuscript. RH and FC confirmed the authenticity of all the raw data. All authors have read and approved the final manuscript.

Ethics approval and consent to participate

Not applicable.

Patient consent for publication

Not applicable.

Competing interests

The authors declare that they have no competing interests.

References

1. Lee AY and Brady MS: Neoadjuvant immunotherapy for melanoma. J Surg Oncol 123: 782-788, 2021.
2. González-Cruz C, Ferrándiz-Pulido C and García-Patos Briones V: Melanoma in solid organ transplant recipients. Actas Dermosifiliogr (Engl Ed) 112: 216-224, 2021.
3. Balch CM, Balch GC and Sharma RR: Identifying early melanomas at higher risk for metastases. J Clin Oncol 30: 1406-1407, 2012.

4. Song Z, Tu X, Zhou Q, Huang J, Chen Y, Liu J, Lee S, Kim W, Nowsheen S, Luo K, *et al*: A novel UCHL3 inhibitor, perifosine, enhances PARP inhibitor cytotoxicity through inhibition of homologous recombination-mediated DNA double strand break repair. Cell Death Dis 10: 398, 2019.
5. Cheng F, Chen H, Zhang L, Li RH, Liu Y and Sun JF: Inhibition of the NEDD8 conjugation pathway by shRNA to UBA3, the subunit of the NEDD8-activating enzyme, suppresses the growth of melanoma cells. Asian Pac J Cancer Prev 13: 57-62, 2012.
6. Cheng F, He R, Zhang L, Li H, Zhang W, Ji X, Kong F, Sun J and Chen S: Expression of neddylation-related proteins in melanoma cell lines and the effect of neddylation onmelanoma proliferation. Oncol Lett 7: 1645-1650, 2014.
7. Jang MJ, Baek SH and Kim JH: UCH-L1 promotes cancer metastasis in prostate cancer cells through EMT induction. Cancer Lett 302: 128-135, 2011.
8. Li G, Jin X, Zheng J, Jiang N and Shi W: UCH-L3 promotes non-small cell lung cancer proliferation via accelerating cell cycle and inhibiting cell apoptosis. Biotechnol Appl Biochem 68: 165-172, 2021.
9. Song HM, Lee JE and Kim JH: Ubiquitin C-terminal hydrolase-L3 regulates EMT process and cancer metastasis in prostate cell lines. Biochem Biophys Res Commun 452: 722-727, 2014.
10. Artavanis-Tsakonas K, Weihofen WA, Antos JM, Coleman BI, Comeaux CA, Duraisingh MT, Gaudet R and Ploegh HL: Characterization and structural studies of the Plasmodium falciparum ubiquitin and Nedd8 hydrolase UCHL3. J Biol Chem 285: 6857-6866, 2010.
11. Rabut G and Peter M: Function and regulation of protein neddylation. 'Protein modifications: Beyond the usual suspects' review series. EMBO Rep 9: 969-976, 2008.
12. Frickel EM, Quesada V, Muething L, Gubbels MJ, Spooner E, Ploegh H and Artavanis-Tsakonas K: Apicomplexan UCHL3 retains dual specificity for ubiquitin and Nedd8 throughout evolution. Cell Microbiol 9: 1601-1610, 2007.
13. Luo K, Li L, Li Y, Wu C, Yin Y, Chen Y, Deng M, Nowsheen S, Yuan J and Lou Z: A phosphorylation-deubiquitination cascade regulates the BRCA2-RAD51 axis in homologous recombination. Genes Dev 30: 2581-2595, 2016.
14. Enchev RI, Schulman BA and Peter M: Protein neddylation: Beyond cullin-RING ligases. Nat Rev Mol Cell Biol 16: 30-44, 2015.
15. Chen JJ, Schmucker LN and Visco DP Jr: Identifying de-NEDDylation inhibitors: Virtual high-throughput screens targeting SENP8. Chem Biol Drug Des 93: 590-604, 2019.
16. Mandelker DL, Yamashita K, Tokumaru Y, Mimori K, Howard DL, Tanaka Y, Carvalho AL, Jiang WW, Park HL, Kim MS, *et al*: PGP9.5 promoter methylation is an independent prognostic factor for esophageal squamous cell carcinoma. Cancer Res 65: 4963-4968, 2005.
17. Song Z, Li J, Zhang L, Deng J, Fang Z, Xiang X and Xiong J: UCHL3 promotes pancreatic cancer progression and chemo-resistance through FOXM1 stabilization. Am J Cancer Res 9: 1970-1981, 2019.
18. Wang G, Zhang W, Zhou B, Jin C, Wang Z, Yang Y, Wang Z, Chen Y and Feng X: The diagnosis value of promoter methylation of UCHL1 in the serum for progression of gastric cancer. Biomed Res Int 2015: 741030, 2015.
19. Seliger B, Handke D, Schabel E, Bukur J, Lichtenfels R and Dammann R: Epigenetic control of the ubiquitin carboxyl terminal hydrolase 1 in renal cell carcinoma. J Transl Med 7: 90, 2009.
20. Mitsui Y, Shiina H, Hiraki M, Arichi N, Hiraoka T, Sumura M, Honda S, Yasumoto H and Igawa M: Tumor suppressor function of PGP9.5 is associated with epigenetic regulation in prostate cancer-novel predictor of biochemical recurrence after radical surgery. Cancer Epidemiol Biomarkers Prev 21: 487-496, 2012.
21. Brait M, Maldonado L, Noordhuis MG, Begum S, Loyo M, Poeta ML, Barbosa A, Fazio VM, Angioli R, Rabitti C, *et al*: Association of promoter methylation of VGF and PGP9.5 with ovarian cancer progression. PLoS One 8: e70878, 2013.
22. Kwon J, Wang YL, Setsuie R, Sekiguchi S, Sakurai M, Sato Y, Lee WW, Ishii Y, Kyuwa S, Noda M, *et al*: Developmental regulation of ubiquitin C-terminal hydrolase isozyme expression during spermatogenesis in mice. Biol Reprod 71: 515-521, 2004.
23. Mtango NR, Sutovsky M, Vandevoort CA, Latham KE and Sutovsky P: Essential role of ubiquitin C-terminal hydrolases UCHL1 and UCHL3 in mammalian oocyte maturation. J Cell Physiol 227: 2022-2029, 2012.
24. Yi YJ, Sutovsky M, Song WH and Sutovsky P: Protein deubiquitination during oocyte maturation influences sperm function during fertilisation, antipolyspermy defense and embryo development. Reprod Fertil Dev 27: 1154-1167, 2015.
25. Miyoshi Y, Nakayama S, Torikoshi Y, Tanaka S, Ishihara H, Taguchi T, Tamaki Y and Noguchi S: High expression of ubiquitin carboxy-terminal hydrolase-L1 and -L3 mRNA predicts early recurrence in patients with invasive breast cancer. Cancer Sci 97: 523-529, 2006.
26. Rolén U, Kobzeva V, Gasparjan N, Ovaa H, Winberg G, Kisseljov F and Masucci MG: Masucci, Activity profiling of deubiquitinating enzymes in cervical carcinoma biopsies and cell lines. Mol Carcinog 45: 260-269, 2006.
27. Hayashi-Nishino M, Fujita N, Noda T, Yamaguchi A, Yoshimori T and Yamamoto A: A subdomain of the endoplasmic reticulum forms a cradle for autophagosome formation. Nat Cell Biol 11: 1433-1437, 2009.
28. Onorati AV, Dyczynski M, Ojha R and Amaravadi RK: Targeting autophagy in cancer. Cancer 124: 3307-3318, 2018.
29. Glick D, Barth S and Macleod KF: Autophagy: Cellular and molecular mechanisms. J Pathol 221: 3-12, 2010.
30. Rubinsztein DC, Codogno P and Levine B: Autophagy modulation as a potential therapeutic target for diverse diseases. Nat Rev Drug Discov 11: 709-730, 2012.
31. Kuma A, Komatsu M and Mizushima N: Autophagy-monitoring and autophagy-deficient mice. Autophagy 13: 1619-1628, 2017.
32. Martinez-Vicente M and Cuervo AM: Autophagy and neurodegeneration: When the cleaning crew goes on strike. Lancet Neurol 6: 352-361, 2007.
33. Kirshenbaum LA: Regulation of autophagy in the heart in health and disease. J Cardiovasc Pharmacol 60: 109, 2012.
34. He C, Bassik MC, Moresi V, Sun K, Wei Y, Zou Z, An Z, Loh J, Fisher J, Sun Q, *et al*: Exercise-induced BCL2-regulated autophagy is required for muscle glucose homeostasis. Nature 481: 511-515, 2012.
35. Yousefi S and Simon HU: Autophagy in cancer and chemotherapy. Results Probl Cell Differ 49: 183-190, 2009.
36. White E: Deconvoluting the context-dependent role for autophagy in cancer. Nat Rev Cancer 12: 401-410, 2012.
37. Choi AM, Ryter SW and Levine B: Autophagy in human health and disease. N Engl J Med 368: 651-662, 2013.
38. Tschan MP and Simon HU: The role of autophagy in anticancer therapy: Promises and uncertainties. J Intern Med 268: 410-418, 2010.
39. Li S, Song Y, Quach C, Guo H, Jang GB, Maazi H, Zhao S, Sands NA, Liu Q, In GK, *et al*: Transcriptional regulation of autophagy-lysosomal function in BRAF-driven melanoma progression and chemoresistance. Nat Commun 10: 1693, 2019.
40. Liu H, He Z and Simon HU: Autophagy suppresses melanoma tumorigenesis by inducing senescence. Autophagy 10: 372-373, 2014.
41. Sivridis E, Koukourakis MI, Mendrinos SE, Karpouzis A, Fiska A, Kouskoukis C and Giatromanolaki A: Beclin-1 and LC3A expression in cutaneous malignant melanomas: A biphasic survival pattern for beclin-1. Melanoma Res 21: 188-195, 2011.
42. Lazova R, Klump V and Pawelek J: Autophagy in cutaneous malignant melanoma. J Cutan Pathol 37: 256-268, 2010.
43. Li JX, Yan Q, Liu N, Zheng WJ, Hu M, Yu ZM, Zhou YD, Wang XW, Liang FX and Chen R: The prognostic value of autophagy-related markers bclin-1 and LC-3 in colorectal cancers: A systematic review and meta-analysis. Evid Based Complement Alternat Med 2020: 8475840, 2020.
44. Li X, He S and Ma B: Autophagy and autophagy-related proteins in cancer. Mol Cancer 19: 12, 2020.
45. Chu Y, Kang Y, Yan C, Yang C, Zhang T, Huo H and Liu Y: LUBAC and OTULIN regulate autophagy initiation and maturation by mediating the linear ubiquitination and the stabilization of ATG13. Autophagy 17: 1684-1699, 2020.